Assessment of Dissolution Kinetics and Buoyant Velocity of Two Different Gases in a Five-meter High Seawater Column

S. Van Ganse and S. Le Floch
Cedre, Centre de documentation, de recherche et d'expérimentations sur les pollutions
accidentelles des eaux, Département Lutte et moyens de lutte - R&D
Brest Cedex 2, France
stephane.le.floch@cedre.fr

Abstract

Further understanding of the fate of oil and gas in the seawater column, when accidentally released in deep water, is required to improve existing numerical models. Many models use a two-equation approach to calculate the terminal velocity of particles (solid, liquid, or gas) by assuming that particles are spherical and rigid. After the Macondo incident, it clearly appeared that this point is not accurate and also that a percentage of gas and oil droplets may dissolve in the water column.

This paper introduces experiments conducted in the Cedre Experimental Column (CEC, a 5 m high and 1m in diameter column filled with seawater) and focus on the fate of gas bubbles in a water column. Attention was given to the motion of the bubbles governed only by the buoyant velocity and not by the jet/plume dynamics. The shadowgraph technique, using high speed video recording, allowed accurate measurement of the particles' velocities, their size and shape, during their transfer to the sea surface.

Following this first set of experiments, some promising results on dissolution kinetics, for two different gases, were obtained in relation to bubble size.

1   Introduction

The offshore exploration and production of oil and gas have increased significantly over the last decade. Subsequently the risks of deep-water spills are also increasing, leading to the development of investigations into models simulating the behaviour of oil and gas, if released from the deep marine environment. The recent Deepwater Horizon spill, occurring at a depth of 1500 m, led to greater attention to the processes regulating the transport of the petroleum (oil and gas) to the surface and its fate.

During a deep-water blow-out, two main stages influence the rise of oil/gas mixture. These stages are well described in a number of papers (Leifer, 2010; Yapa et al., 2012).

First, due to the discharge conditions and the ambient conditions, the oil/gas rises as a jet and is governed by plume mixing. This stage is also known as momentum driven jets. The second stage is reached once the plume momentum and seawater entrainment have dissipated. It is governed by the buoyancy of individual oil particles and gas bubbles. For blow-outs occurring at great depth, the gaseous phase and liquid hydrocarbon phase will rise separately depending on the conditions (Yapa and Chen, 2004). Also, in specific conditions, combining high pressure and cold temperature, the gaseous phase, is transformed into gas hydrate (Joye et al., 2011). Furthermore, to model the fate of oil and gas in the water column, the dissolution process in the water column is an essential point (Reddy et al., 2012).

The experiments introduced in this paper focused on the behaviour of individual gas bubbles in a five-meter high seawater column. The shadowgraph technique, used in these experiments, allows the visualization and the characterization of the particles' ascension. The presented experimental data on terminal velocity and dissolution of gas bubbles, gives promising information to improve numerical models simulating the fate of oil and gas in the deep marine environment.

2   Technical Equipment and Method

2.1   The Cedre Experimental Column

The Cedre Experimental Column (CEC) is equipped with an injection system, on which it is possible to fit different diameters of nozzles, and two high speed video recording systems. The CEC is a five-meter high hexagonal column with a diameter of 1m, and a total capacity of 4.50 m^3. The experimental design, presented in Figure 1, is described by Le Floch and Benbouzid (2009). The first camera is located 15 cm above the injection nozzle (3.75 m depth), at a pressure of 141325 Pa. The second camera is located 15 cm below the surface (0.15 m depth and 3.75m above the injection nozzle), at a pressure of 102825 Pa. The distance between the 2 recording systems is 3.60 m. During the experiments the temperature was 784.15 K.
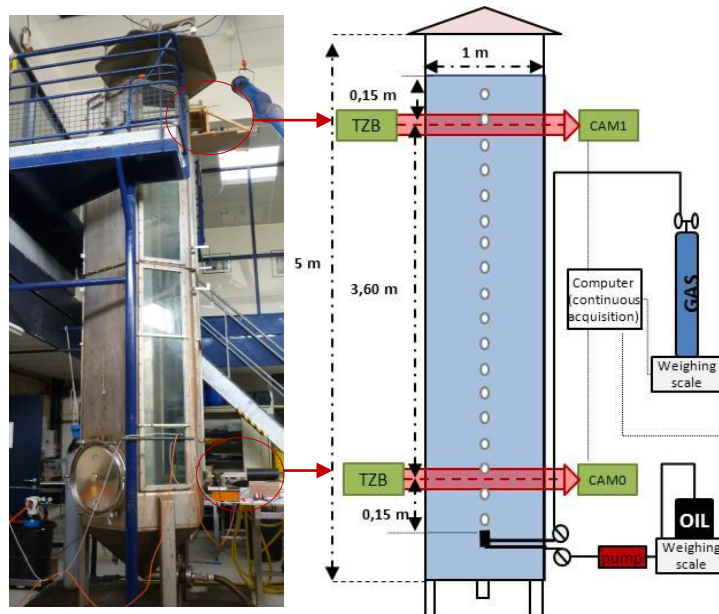

Figure 1. Cedre Experimental Column designed with shadowgraphy equipment (2 lights and cameras on a parallel plane) and bubble injection system of gas and/or oil from the bottom (4 m depth).

2.2   Gas Injection

Air and nitrogen gases have been used in this research in order to study their behaviour differences. Nitrogen was selected as slightly a soluble gas and air was selected as a more soluble gas than nitrogen. Their physico-chemical properties are presented in Table 1. The injection, performed at a depth of 3.90m, is realised by two 50 cm long stainless steel injection tubes combined with a nozzle. One of the injection systems is linked to a pump for oil or air, and the other stainless steel tube is linked to a bottle of gas (nitrogen or air). In order to create different oil droplet or bubble sizes, the nozzle diameter is changed (diameters between 1 mm and 12 mm). To measure the injection flow rate of nitrogen gas, the weight of the gas bottle is continuously recorded for one hour (2 weight readings per second); the resulting curve gives the flow rate (µg/s).

Table 1. Physico-chemical properties of tested gases.

Substance	Density (at 10°C)	Refraction indice (Sodium D line at 20°C)	Interfacial tension with seawater (10°C; atm pressure)
Nitrogen	1.185	1,000297	71,43
Air	1.2929	1,0002926	74.97

LeFloch, S., and S. Van Ganse, Assessment of Dissolution Kinetics and Buoyant Velocity of Two Different Gases in a Five-meter High Seawater Column, Proceedings of the Thirty-sixth AMOP Technical Seminar on Environmental Contamination and Response, Environment Canada, Ottawa, ON, pp. 37-45, 2013.

2.3 High-speed Shadowgraph Visualisation

The experiments performed in the CEC are conducted using the shadowgraph approach. This optical technique, based on the visualization of the variation of refraction indices, reveals non-uniformities in transparent media (Selltes, 2001; Fuhrer et al, 2011). Vicolux TZB95 telecentric lights provides continuous red light illumination and a Nikkor lens 105mm-SVS340 CAM0 and CAM1) records the event. The cameras record at 64 images.s[-1] with a resolution of 640 x 840 pixels. The area of interest (centre of the column), represents 3.42 x 2.57 cm, for CAM0 (bottom) and 2.46 x 1.85 cm for CAM1 (surface) corresponding respectively to a pixel resolution of 53.5 µm and 38.5 µm. Each test was recorded for 1.5 min, and the results take the form of a sequence of images of the bubbles/droplets in the seawater.

Each sequence of images was processed to locate and track the gas bubble with the support of the NI-vision software. Based on the detection of differences of grey levels for each pixel on the images, the bubble (dark) was isolated from the background (bright). The resulting binary images are introduced in Figure 2. This figure shows 8 images of the rise of a nitrogen bubble, where the time separating the first and the last picture is 109 milliseconds (ms). The time separating 2 images is 15.6 ms, and the position of the centre of the bubble on the X and Y axes of the image, allow the bubble velocity (m.s^{-1}) to be calculated. The waddel disk diameter, defined as the diameter of the disk with the same area as the particle[1], is used to calculate the gas volume and the dissolution kinetics.
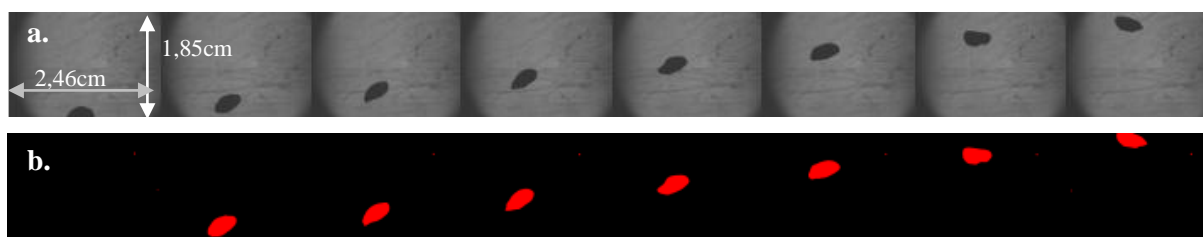

Figure 2. Ascension of a nitrogen bubble, with an acquisition rate of 64 image.s[-1] by the shadowgraph technique (a) and the resulting binary images (b). The time spent between the first and the last image is 109 ms.

2.4 The Seawater

The seawater used to fill the column is taken from the bay of Brest. Before being used it is filtered to remove particles over 25 µm in suspension, and is treated with UV (25 mJ.cm^{-2}) rays. These treatments prevent flocculation between the substances injected and the suspended matter, preventing/limiting interferences with dissolution kinetics. This seawater has a salinity of 35 kg m^{-3} and the temperature during the tests is 284.15 K. The refractive index of the seawater is 1.34 (Copin-Montégut 2002).

3 Results and Discussion
3.1 Influence of the Injection Flow Rate on the Bubble Size and Terminal Velocity

The slip velocity, consisting, in a bubble plume, in the velocity difference between rising bubbles and the surrounding liquid, is dependent on the bubble size (Zheng and Yapa, 2000). Thus, to be sure to consider only the size influence of isolated bubbles, on the terminal velocity in stagnant liquid, the first step is to establish the ideal flow rate conditions.

To evaluate the flow rate impact on the bubble size and terminal velocity, 7 different flow rates of air where tested between 5ml/min[-1] and 60 mL.min^{-1}. Figure 3 shows the terminal velocities and the corresponding equivalent diameters measured for the different

---

[1] $2\sqrt{\text{particle area}}/\sqrt{\Pi}$

flow rate conditions close to the injection outlet (3.9 m depth) and 3.60 m above it. Near the injection outlet, when the injection rate (outlet pressure) increases, the bubble size and the associated velocity increase, from 22.8 ± 1.1 cm.s^{-1} for an equivalent bubble diameter of 4.4 ± 0.1 mm, to a maximum velocity of 28.2 ± 0.7 cm. s^{-1} for an equivalent diameter of 5.0 ± 0.4 mm. Further up the water column, 3.60m above the injection outlet, a slight increase in the equivalent diameter and the terminal velocity is observed, as the flow rate increases until a peak reached at 2350 rpm. At this flow rate, the maximum terminal velocity is 26.9 ± 1.8 cm.s^{-1} for an equivalent bubbles diameter of 5.4 ± 0.3 mm. The decrease in the velocity observed after this point may be explained by the distance between the bubbles during the ascension. The distance between the rising bubbles is known to affect their terminal velocity (Castillejos and Brimacombe, 1987).

The results of the influence of the vertical distance separating bubbles on their velocity are presented in Figure 4. These results are obtained close to the injection nozzle, it was technically not possible to produce the same analysis 3.75 m above it (close to the surface) because, during their ascension, the bubbles may separate horizontally and may not be visible on the recorded images.
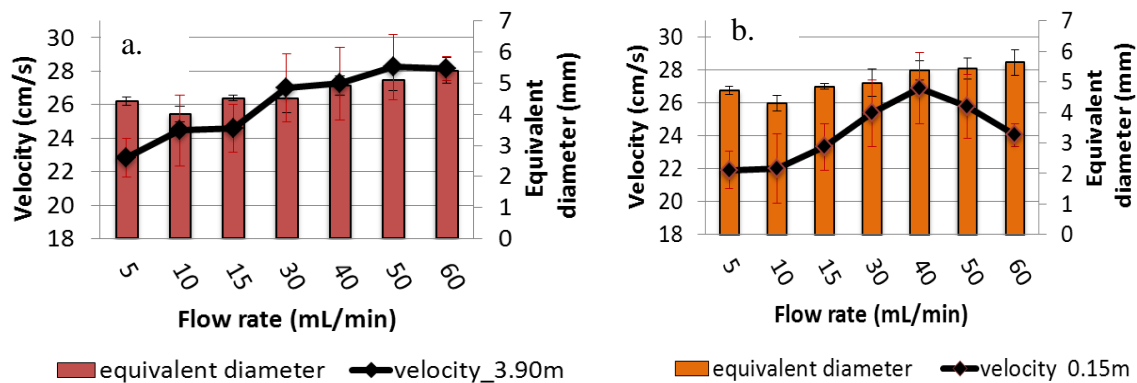

Figure 3. Terminal velocity (cm/s) and equivalent diameter (mm) of the bubbles measured at 3.9 m depth (a) and 0.15 cm depth (b).
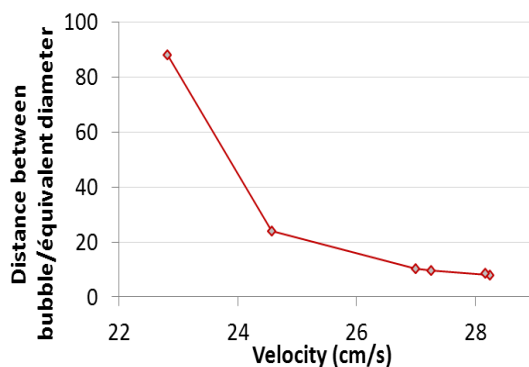

Figure 4. Influence of the vertical distance between the bubbles/equivalent diameter ratio on the terminal velocity (cm/s) of the bubbles.

Figure 4 shows that the distance between the gas bubble has an impact on the measured velocity. The correlation between the increase in the terminal velocity and the

LeFloch, S., and S. Van Ganse, Assessment of Dissolution Kinetics and Buoyant Velocity of Two Different Gases in a Five-meter High Seawater Column, Proceedings of the Thirty-sixth AMOP Technical Seminar on Environmental Contamination and Response, Environment Canada, Ottawa, ON, pp. 37-45, 2013.

decrease of the vertical distance/eq. diameter ratio is shown on the graph. This graph shows that when the distance between bubbles is less than 24 time the equivalent diameter the velocity measured is not corresponding the motion of an individual bubble but is linked with the motion of the bubbles above. This graph, does not show clearly the intermediate stage between the momentum-motion and the buoyant-motion, at which terminal bubble velocities is are not affected by the turbulence fields from the other bubbles. This result need to be studied in further experiments in order to assign the buoyant velocity in numerical models predicting the rise of the gas to the surface depending on the bubble size and also the distances between bubbles.

3.2   Bubble Terminal Velocity

The terminal velocity of an isolated gas bubble is influenced by the equivalent diameter (d), the gravity (g), the mass density of the liquid phase (ρ_l), the difference in mass density between the two phases ($\Delta\rho$); the dynamic viscosity (μ) and the interfacial tension (σ) of the gas and the liquid. An integral approach, well described by Zheng and Yapa (2000), outlines an integrated formula to calculate the buoyant velocity of bubbles/particles. The theoretically based equations describe the velocity of three size ranged bubbles (spherical, ellipsoidal, spherical cap).

In this experiment, the influence of the diameter of the gas bubble has been described for nitrogen gas and air. To be sure that the flow rate does not affect the measurement, the minimal distance between two bubbles is 40 cm (equivalent diameter/vertical distance ratio less than 0.01). Figure 5 shows different regimes of terminal velocity depending on the equivalent bubble diameter for nitrogen gas. The first part of the curve describes the velocity of spherical shape bubbles. In the second part of the curve, the bubbles are characterised by an ellipsoidal shape and the terminal velocity follows a new equation. For the nitrogen gas, the diameter between spherical and ellipsoidal regime (critical diameter) is 1.5 mm. This behaviour is well described in the Clift's paper (Clift et al., 1978) and gives a new numerical approach who integrate size and shape factor of the bubble to calculate the terminal velocity.
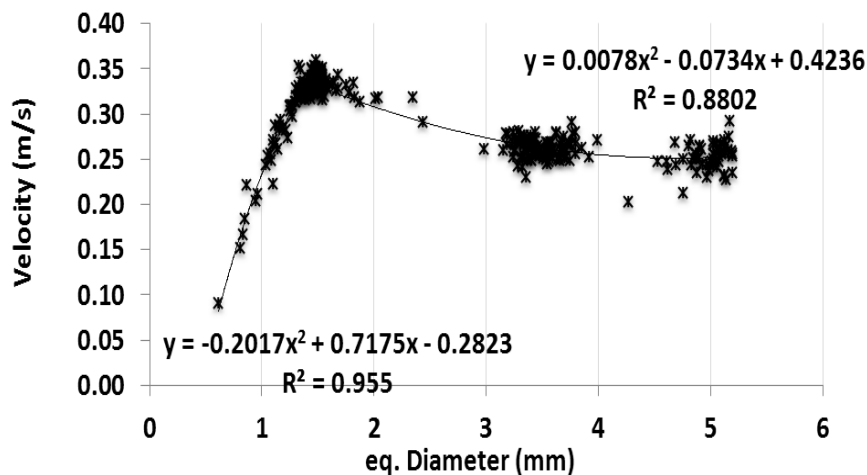

Figure 5 Terminal velocity (m/s) of Nitrogen bubbles in seawater a 10°C.

Figure 6 presents preliminary results for air bubble velocity. The group of points correspond to the regime characterised by spherical bubbles (eq. diameter<1.1 mm). The second group of points correspond to the ellipsoidal regime (3.4 mm<eq. diameter<6.2 mm).

Intermediate points are missing in this figure to conclude on the critical diameter at which the bubble are switching from spherical shape to ellipsoidal shape.
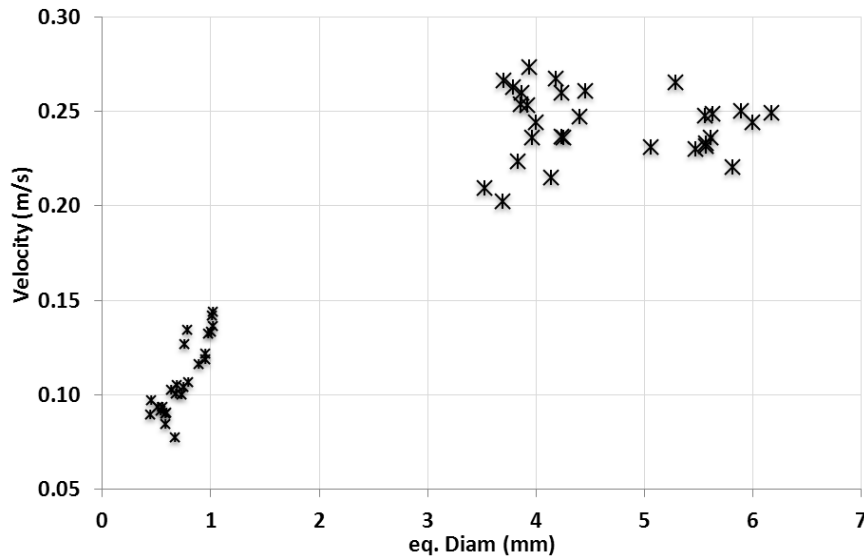
3.3   Gas Dissolution in the Water Column

The dissolution rate of chemical substances, oil or gases is generally studied by quantifying the product in water (Arey et al., 2007). In this experiment the dissolution was measured by calculating the difference in volume of the bubble at 3.9 0mdepth and 0.25 m.

Figure 7 shows the nitrogen equivalent diameter for bubbles obtained at 3.9 0m depth and 0.15 m depth using different nozzle diameters. The bubble size increased during the ascension due to the decrease in pressure in the water. The mean percentage rate volume increase per meter for nitrogen gas was 2.6%, and for air was 2.0%. These results can be explained by the different dissolution rates of the gases.

Considering that the two studied gases behave like ideal gas in the water column, the ideal gas law is used as followed:

$$PV = nRT$$

The numbers of moles are obtained at each depth by:

$$n = \frac{PV}{RT}$$

with R, ideal gas constant: 8,31 $Pa.m^3.mol^{-1}.kg^{-1}$
V, volume at 3.9 0 m depth or 0.15 m depth.
P, pressure at 3.9 0 m depth: 141325 Pa and 0.15 m depth: 102825 Pa
T, temperature: 784.15 K

The number of dissolved moles are calculated by the difference between the moles calculated at 3.9 0m depth and the moles calculated at 0.15 m depth.

LeFloch, S., and S. Van Ganse, Assessment of Dissolution Kinetics and Buoyant Velocity of Two Different Gases in a Five-meter High Seawater Column, Proceedings of the Thirty-sixth AMOP Technical Seminar on Environmental Contamination and Response, Environment Canada, Ottawa, ON, pp. 37-45, 2013.
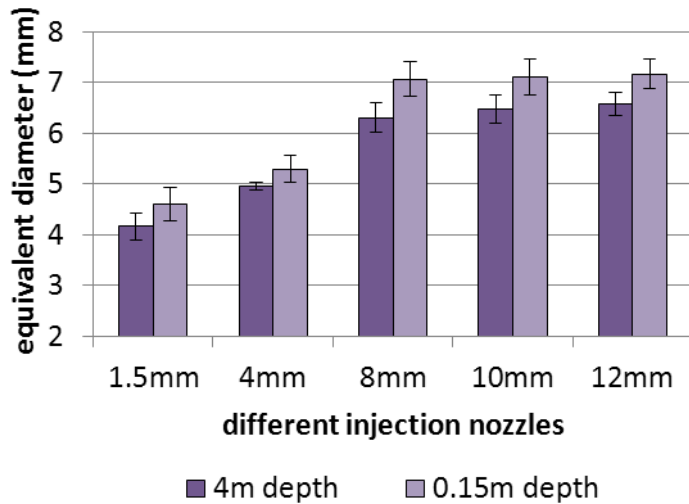
Figure 5. Nitrogen bubble equivalent diameter (mm) obtained

with different injection diameters (1.5 mm to 12 mm)

Figure 8 presents the percentage of dissolved moles per meter according to the equivalent diameter. The dissolution of the air is higher than the dissolution of the nitrogen for bubbles of the same size. Also, the dissolution of air seems to increase linearly with the increase in bubble size, contrary to the nitrogen gas. The nitrogen does not present a significant tendency between dissolution and equivalent diameter. This experiment needs to be continued with more experiments to reinforce these results statistically.
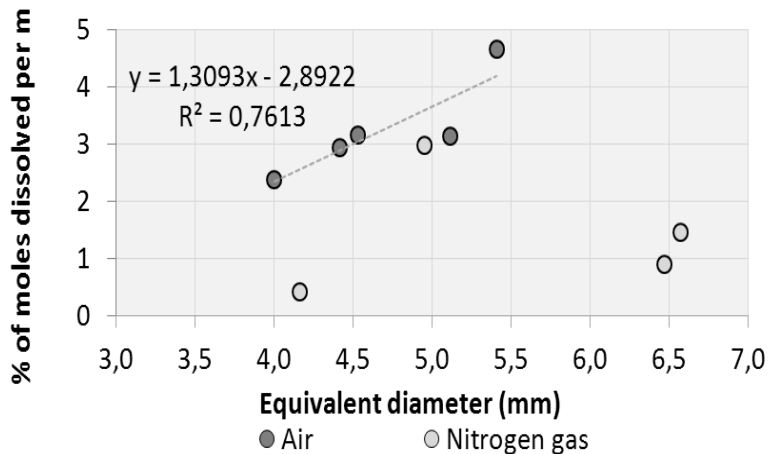

Figure 6. Percentage of dissolved moles of nitrogen and air per meter

depending on bubble size (equivalent diameter).

4   Conclusion and Future Prospects

The introduced initial results of on-going experiments on gas slip velocity and dissolution (on nitrogen gas and air), with the use of a five-meter high water column,

demonstrate that the buoyant velocity of bubbles is dependent on the size and also the shape of the bubble and that the dissolution may affect the bubble. These two points cannot be ignored in models simulating the fate of oil and gas plumes. When a blowout occurs in deep water, gas bubbles have a wide range of sizes, and may also be affected by physical modification like hydrates. Dissolution may also affect the bubbles sizes and the rate of petroleum (gas and oil) rising to the surface.

Current models are mainly based on theoretical equations and do not always consider every process occurring on oil and gases rising from deep water. The experiment data presented in this paper demonstrates that theoretical predictions have limits. Also, the Deepwater Horizon (DWH) event confirmed that models do not always fit with real life conditions and some processes may be considered to a lesser extent, like dissolution rate, slip velocity of particles or hydrate formation.

To follow this paper, new experiments on hydrocarbon gases (CH_4 to C_4H_{10}) would be beneficial to produce a prediction of slip velocity and dissolution rate of gases coming from drilling operations in deep water. This type of experimental data would be useful to improve current numerical models. The study of interaction between gas and oil would also give answers to the separation probability of oil and gas in deep water. Furthermore, knowing that gas rises more rapidly to the surface, and considering the observation that some oil may be fixed to the gas bubble (forming "oily bubbles") as it rises, it would be suitable to investigate how different ratios of oil and gas impact the rise velocity in the water column. Also, since the gases from drilling are highly explosive, the resulting data would also be of interest for safety procedures at the surface of drilling operating units.

5   References

Arey, J.S., R.K. Nelson, D.L. Plata, and C.M. Reddy, "Disentangling Oil Weathering Using GC+GC.2 Mass Transfer Calculations", *Environment Science Technology*, 41: 5747-55, 2007.

Castillejos, A.H. and J.K. Brimacombe, "Measurement of Physical Characteristics of Bubbles in Gas-Liquid Plumes Part 2. Local Properties of Turbulent Air-Water Plumes", *Vertically Injected Jets. Metallurgical Transaction B*, Vol.18b, pp. 659-671, 1987.

Clift, R., J.R. Grace, and M.E. Weber, *Bubbles, Drops and Particles*, Academic Press, New York, 1978.

Joye, S.B., I.R. MacDonald, I. Leifer, and V. Asper, "Magnitude and Oxidation Potential of Hydrocarbon Gases Released from BP Oil Well Blowout", *Nature Geoscience*, Vol. 4, 2011.

Fuhrer, M., P. Slangen, L. Aprin, G. Dusserre, and S. Le Floch, "A New Approach to Analyze Chemical Releases Behavior in Water Column: High Speed Imaging", *Proceedings of 2011 International Oil Spill Conference (IOSC)*, Portland, Oregon, USA, 23-26 May, 21, 2011.

Le Floch, S., H Benbouzid, et al. "Operational Device and Procedure to Test Initial Dissolution Rate of Chemicals after Ship Accidents: The Cedre Experimental Column", *The Open Environmental Pollution & Toxicology Journal*, 1:1-10, 2009.

Leifer, I., "Charactrtistics and Scaling of Bubble Plumes from Marine Hydrocarbon Seepage in the Coal Oil Point Seep Field", *J. Geophys.Res.* 115, C11014, doi: 10.1029/2009JC005844, 2010.

Li, Z. and P.D. Yapa,"Buoyant Velocity of Spherical and Non-spherical Bubbles/Droplets", *Journal of Hydraulic Engineering*, Members ASCE, 126:852-854, 2000.

Reddy, C.M., J.S. Arey, J.S. Seewald, S.P. Sylva, K.L. Lemkau, R.K. Nelson, C.A. Carmicheal, C.P. Mclntyre, J. Fenwick, G.T. Ventura, B.A.S. Van Mooy, and Richard Camilli, "Composition and Fate of Gas and Oil Released to the Water Column during the *Deepwater Horizon* Oil Spill", *PNAS*, Vol. 109, No. 50, pp. 20229-20234, 2012.

Settles, G.S., *Schieren and Shadowgraph Techniques: Visualizing Phenomena in Transparent Media*, Springer Verlag, 2001.

Yapa, P.D. and F. Chen, "Behavior of Oil and Gas from Deepwater Blowout", *Journal of Hydraulic Engineering*, 130:540-553, 2004.

Yapa, P.D., M.R. Wimalaranta, A.L. Dissanayake, J.A. Degraff Jr., "How Does Oil and Gas Behave when Released in Deepwater?", *Journal of Hydro-environment Research,* pp. 6257-6285, 2012.

LeFloch, S., and S. Van Ganse, Assessment of Dissolution Kinetics and Buoyant Velocity of Two Different Gases in a Five-meter High Seawater Column, Proceedings of the Thirty-sixth AMOP Technical Seminar on Environmental Contamination and Response, Environment Canada, Ottawa, ON, pp. 37-45, 2013.